Optomechanically Induced Transparency in the Nonlinear Quantum Regime

Andreas Kronwald[1, *] and Florian Marquardt[1, 2]

[1]*Friedrich-Alexander-Universität Erlangen-Nürnberg, Staudtstr. 7, D-91058 Erlangen, Germany*
[2]*Max Planck Institute for the Science of Light, Günther-Scharowsky-Straße 1/Bau 24, D-91058 Erlangen, Germany*

Optomechanical systems have been shown both theoretically and experimentally to exhibit an analogon to atomic electromagnetically induced transparency, with sharp transmission features that are controlled by a second laser beam. Here we investigate these effects in the regime where the fundamental nonlinear nature of the optomechanical interaction becomes important. We demonstrate that pulsed transistor-like switching of transmission still works even in this regime. We also show that optomechanically induced transparency at the second mechanical sideband could be a sensitive tool to see first indications of the nonlinear quantum nature of the optomechanical interaction even for single-photon coupling strengths significantly smaller than the cavity linewidth.

Introduction – Optomechanics explores the coupling between photons and phonons via radiation pressure. It aims at applications in classical and quantum information processing as well as ultrasensitive measurements and tests of fundamental quantum effects using mesoscopic or macroscopic systems [1, 2]. Recently, a feature called "optomechanically induced transparency" (OMIT) has been predicted theoretically [3] and observed experimentally [4–6]: The photon transmission through an optomechanical cavity is drastically influenced when introducing a second laser beam. This leads to the appearance of very sharp features in the transmission signal, which can be controlled by the second beam. OMIT can thus be employed for slowing and stopping light or for operating a "transistor", where photon transmission is switched on and off optically [3, 4, 6, 7]. OMIT is an analogon of atomic electromagnetically induced transparency [8], where a medium consisting of three-level atoms can be made transparent by illuminating it with a second laser.

The optomechanical interaction is fundamentally nonlinear at the quantum level. However, in most optomechanical systems the coupling between single photons and phonons is small compared to dissipation rates (except in cold atom clouds [9–11], which have other constraints). It will therefore be extremely challenging to detect effects of this nonlinearity on the quantum level. Indeed, all the optomechanical quantum phenomena observed so far can be described in a simpler linear model, where the coupling is effectively enhanced via the photon number.

Nevertheless, experiments are recently making progress in increasing the coupling strength [12–15], coming closer to the nonlinear quantum regime. That regime has attracted large theoretical interest leading to the prediction of optical Schrödinger cat states [16, 17], a classical to quantum crossover in nonlinear optomechanical systems [18], non-Gaussian [19] and nonclassical mechanical states [20–22], as well as multiple cooling resonances [23]. Certain dark states [24], photon antibunching [25, 26], a crossover from sub-Poissonian to super-Poissonian statistics and photon cascades [26] may
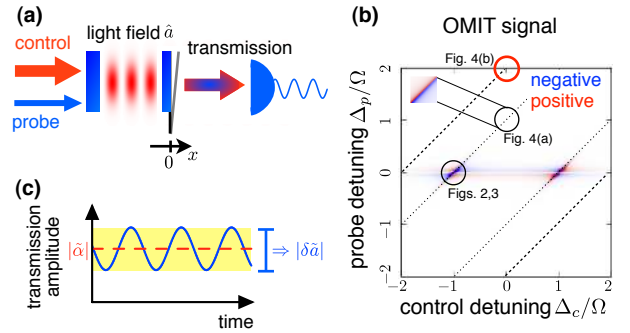

Figure 1: (a) Standard optomechanical setup driven by a control and a probe laser. (b) Classical expectation of the OMIT signal as a function of the probe and control detuning, cf. Eq. (6). If the beat frequency of the two lasers $|\omega_c - \omega_p| \sim \Omega$, a signal is expected (dotted, black lines). We study the OMIT signal at the circles. In particular, we find an OMIT signal at the second mechanical sideband (red, thick circle) even at moderate single-photon coupling, where a classical analysis fails to show the signal. This is a clear signature of the optomechanical quantum nonlinearity. (c) Field amplitude in a frame rotating at the control laser frequency ω_c. The control generates a constant transmission amplitude $\tilde{\alpha}$ (red, dashed line). The probe induces oscillations at the beat frequency $\omega_p - \omega_c$. The amplitude of these oscillations, Eq. (4), is our signal. [Parameters: $g = g_0 |\alpha| = 0.08\,\Omega$, $\kappa = \Omega/8$, $\Gamma_M = 0.01\,\Omega$].

be observed. Two-mode setups [27, 28] and collective effects in optomechanical arrays [29] have been shown to be favorable for reaching strong quantum nonlinearities.

In this paper, we go beyond the classical analysis of OMIT [3, 4, 30, 31] and analyze OMIT in the nonlinear quantum regime. By simulations of the full quantum dissipative dynamics, we study the spectroscopic signal and the time-evolution during pulsed operation. In analyzing OMIT at mechanical sidebands, we find that OMIT could be a crucial tool to observe first tell-tale effects of the nonlinear quantum regime even for single-photon coupling strengths much smaller than the cavity linewidth,

in contrast to the standard single-beam situation [19, 25].

Model – We consider a generic optomechanical system, where an optical cavity is coupled to mechanical motion, cf. Fig. 1(a). The system's Hamiltonian reads [32]

$$\hat{H} = \hbar\omega_{\mathrm{cav}}\hat{a}^\dagger\hat{a} + \hbar\Omega\hat{b}^\dagger\hat{b} - \hbar g_0\left(\hat{b}^\dagger + \hat{b}\right)\hat{a}^\dagger\hat{a} + \hat{H}_{\mathrm{dr}}, \quad (1)$$

where $\hat{a}$ ($\hat{b}$) is the photon (phonon) annihilation operator, ω_{cav} (Ω) the cavity (mechanical) resonance frequency, and g_0 the optomechanical coupling between single photons and phonons. $\hat{H}_{\mathrm{dr}}$ describes the two-tone driving,

$$\hat{H}_{\mathrm{dr}} = \hbar\left[\varepsilon_c e^{-\mathrm{i}\omega_c t} + \varepsilon_p e^{-\mathrm{i}\omega_p t}\right]\hat{a}^\dagger + \mathrm{H.c}, \quad (2)$$

where ω_c (ω_p) and ε_c (ε_p) are the control (probe) laser frequency and amplitude, respectively. In order to neglect other mechanical resonances, one has to assume $g_0 \ll \Omega$. We also assume near-resonant excitation (and narrow-band detection) of the mechanical sidebands under consideration.

The optomechanical interaction can be diagonalized (for $\varepsilon_{c,p} = 0$) by shifting the mechanical equilibrium position by $\delta x \propto 2n_a g_0/\Omega$ depending on the photon number n_a ("polaron transformation") [16, 17]. This will allow us to understand OMIT in terms of interference pathways in the resulting level scheme. The corresponding eigenstates read $|n_a, n_b\rangle$ where n_a (n_b) is the number of photons (phonons in the shifted frame). The eigenenergies read $E\left(n_a, n_b\right)/\hbar = \omega_{\mathrm{cav}}^{\mathrm{eff}}n_a + \Omega n_b - g_0^2 n_a\left(n_a - 1\right)/\Omega$ [16, 17], where $\omega_{\mathrm{cav}}^{\mathrm{eff}} = \omega_{\mathrm{cav}} - g_0^2/\Omega$ is the effective cavity resonance frequency. The control/probe detuning from $\omega_{\mathrm{cav}}^{\mathrm{eff}}$ is defined as $\Delta_{c/p} = \omega_{c/p} - \omega_{\mathrm{cav}}^{\mathrm{eff}}$.

Dissipative Dynamics – The dissipative dynamics for weak optomechanical coupling can be described by a Lindblad master equation

$$\dot{\hat{\rho}} = \frac{\mathrm{i}}{\hbar}\left[\hat{\rho}, \hat{H}\right] + \kappa\mathcal{D}[\hat{a}]\hat{\rho} + \Gamma_M\left(n_{\mathrm{th}} + 1\right)\mathcal{D}[\hat{b}]\hat{\rho} + \Gamma_M n_{\mathrm{th}}\mathcal{D}[\hat{b}^\dagger]\hat{\rho}. \quad (3)$$

$\hat{\rho}$ denotes the density matrix for the optical and mechanical mode. κ is the photon loss rate (due to loss through both, input *and* output mirror), and Γ_M the phonon decay rate. n_{th} is the thermal occupancy of the mechanical bath and $\mathcal{D}\left[\hat{A}\right]\hat{\rho} = \hat{A}\hat{\rho}\hat{A}^\dagger - \hat{A}^\dagger\hat{A}\hat{\rho}/2 - \hat{\rho}\hat{A}^\dagger\hat{A}/2$ is the Lindblad dissipation superoperator. We solve (3) in the time-domain numerically. This allows to also consider pulse-based schemes.

Two-tone transmission – In the steady state, the intra-cavity field amplitude in a frame rotating at the control frequency ω_c is defined by

$$\langle\hat{a}\rangle = \alpha + \varepsilon_p\left[\delta a_1 e^{-i(\omega_p - \omega_c)t} + \delta a_{-1} e^{i(\omega_p - \omega_c)t}\right]. \quad (4)$$

The control beam induces a constant amplitude α, whereas $\delta a_{\pm 1}$ are two (first-order) sidebands due to the probe. Higher harmonics of the beat frequency $\omega_p - \omega_c$ are also present due to the nonlinear interaction. However, they are weak in our analysis and have been omitted in (4).

The experimentally accessible transmitted field amplitude $\langle\hat{a}_{\mathrm{out}}\rangle$ is related to the cavity field (4) by the input-output relation $\langle\hat{a}_{\mathrm{out}}\rangle = \sqrt{\kappa_O}\langle\hat{a}\rangle$ [33], where κ_O is the output mirror decay rate. In the following, we analyze what we term the normalized probe beam transmission

$$|\delta\tilde{a}|^2 = \kappa_O\varepsilon_p^2\left(|\delta a_1|^2 + |\delta a_{-1}|^2\right)/|\delta a_{\mathrm{out}}^{\mathrm{max}}|^2. \quad (5)$$

This is essentially the intensity transmitted at the probe beam frequency ω_p and at the other sideband, $2\omega_c - \omega_p$, divided by the incoming probe intensity $|\delta a_{\mathrm{out}}^{\mathrm{max}}|^2 = \kappa_O \cdot 4\varepsilon_p^2/\kappa^2$. $|\delta a_{\pm 1}|$ can be measured via heterodyning [34], i.e. mixing $\hat{a}_{\mathrm{out}}$ with a local oscillator at ω_c and obtaining the power in the signal at $\omega_p \pm \omega_c$.

To isolate signatures in the probe beam transmission which emerge due to the presence of the control beam, we introduce the "OMIT signal". It is defined as the difference of $|\delta\tilde{a}|^2$ with and without control laser.

Standard prediction – OMIT has so far been studied only in the *linearized* regime of optomechanics, where the quantum nonlinearity is neglected. In this regime, the OMIT signal depends only on the product $g_0|\alpha|$ of the coupling and the intra-cavity field amplitude $\alpha = i\varepsilon_c/\left(i\Delta_c - \kappa/2\right)$. For this to be valid, $g_0 \ll \kappa$.

We recall that a common OMIT signature arises when the control laser drives the cavity on the red sideband, i.e. $\Delta_c = -\Omega$. The probe beam transmission as a function of the probe detuning Δ_p then shows a transmission dip on resonance (i.e. $\Delta_p = 0$), cf. Fig. 2(b). The dip's width is $\Gamma_M + \Gamma_{\mathrm{opt}} \ll \kappa$ (with $\Gamma_{\mathrm{opt}} = 4g_0^2|\alpha|^2/\kappa$). The normalized probe beam transmission reads [3, 30]

$$|\delta\tilde{a}|^2 = \frac{\kappa^2}{4}\left|\frac{1}{-i\Delta_p + \frac{\kappa}{2} - 2i\frac{g_0^2}{\Omega}|\alpha|^2\chi[\omega_p - \omega_c]}\right|^2, \quad (6)$$

where $\chi^{-1}[\omega] = 1 - (\omega/\Omega)^2 - i\omega\Gamma_M/\Omega^2$ is the (rescaled) mechanical susceptibility.

If $\Delta_p \approx 0$, the beat frequency $\omega_p - \omega_c$ between probe and control is given by the mechanical frequency Ω. Thus, the mechanical resonator is driven by a force oscillating at its eigenfrequency and the resonator starts to oscillate coherently. This motion induces sidebands on the cavity field, generating photons with frequency ω_p. These interfere destructively with the probe beam, leading to a transmission dip. Typically, OMIT has been studied in a regime where $\Gamma_M \ll \Gamma_{\mathrm{opt}}$ and $g_0|\alpha| \ll \kappa \ll \Omega$ [4–6], such that the OMIT dip's width is $\sim \Gamma_{\mathrm{opt}}$.

We now focus on the regime where the quantum nonlinearity becomes important. Quantum nonlinear features can be unambiguously distinguished from classical effects (or linear quantum effects) by studying their dependence
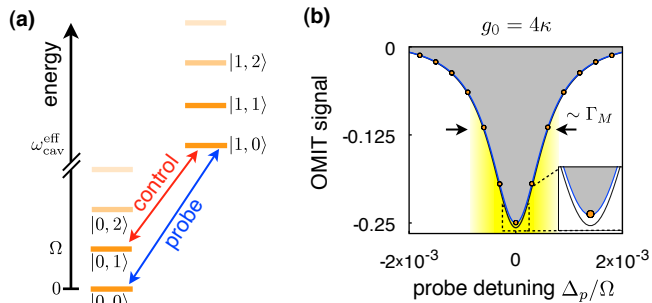
Figure 2: Quantum nonlinearities and OMIT. (a) Energy level scheme of the optomechanical system with levels $|n_a, n_b\rangle$, cf. main text. n_a (n_b) denotes the number of photons (phonons). Here, for example, the probe couples $|0,0\rangle \leftrightarrow |1,0\rangle$ since the detuning $\Delta_p = \omega_p - \omega_{\text{cav}}^{\text{eff}} = 0$. The control couples $|0,1\rangle \leftrightarrow |1,0\rangle$ since $\Delta_c = \omega_c - \omega_{\text{cav}}^{\text{eff}} = -\Omega$. (b) The OMIT signal. Orange circles: Numerical results for $g_0/\kappa = 4$. Black line: Expectation for the standard, classical regime, Eq. (6). Blue line: Expectation of Eq. (6), but including Franck-Condon factors and $|\alpha|^2 \to \langle \hat{a}^\dagger \hat{a}\rangle$, see main text. [Parameters: $\kappa = \Omega/40$, $\Gamma_M = 10^{-3}\,\Omega$, $\varepsilon_c = 10^{-2}\,\Omega$, $\Delta_c = -\Omega$, $n_{\text{th}} = 0$].

on the "quantum parameter" g_0/κ [9, 18]. Let us imagine that Planck's constant $\hbar \to 0$. In this limit, all classical effects remain while all quantum effects become vanishingly small. In the context of optomechanics, varying $\hbar$ is equivalent to keeping all classical parameters $(\Delta, \kappa, \ldots)$ fixed while tuning the "quantum parameter" $g_0/\kappa \propto \sqrt{\hbar}$ [2, 9, 18]. As $g_0 \to 0$, we increase the laser power ε_c, hence $g_0 |\alpha| = \text{const}$. This retains the size of the classical OMIT signal, cf. (6). In contrast, any truly quantum-mechanical nonlinear effects vanish as $g_0 \to 0$. Note that for our parameters, a *single* photon can have a large impact [19, 25], so we limit ourselves to weak laser driving, i.e. $\varepsilon_p, \varepsilon_c \ll \kappa$ (thus $|\alpha| \ll 1$) in contrast to the standard OMIT scenario, where $\epsilon_{p,c}$ can be arbitrary. This also implies that the OMIT dip's width is $\sim \Gamma_M$.

Main OMIT dip – To compare against *classical* OMIT predictions, we first focus on the OMIT dip at resonance, while keeping the full nonlinear *quantum* interaction of (1), cf. Fig. 2(b). Consider the level scheme of Fig. 2(a). Since both lasers are assumed to be weak, only the zero and one photon ladders are important. We again assume $\Delta_c = -\Omega$, such that the control hybridizes the states $|0,1\rangle \leftrightarrow |1,0\rangle$. This leads to a destructive interference of the two probe excitation pathways at $\Delta_p = 0$ and thus the OMIT dip.

The most important change in the OMIT signal is that the main OMIT dip's depth is modified due to shifted phonon states: The probe laser drives the transition $|0,0\rangle \leftrightarrow |1,0\rangle$ resonantly, i.e. the transition of a 0-phonon state and a *shifted* 1-phonon state. This leads to the Franck-Condon factor $\exp[-(g_0/\Omega)^2]$ which will enter the numerator of (6) [19]. Also, the photon number $\langle \hat{a}^\dagger \hat{a}\rangle$ ($|\alpha|^2$ in the classical theory) entering the de-
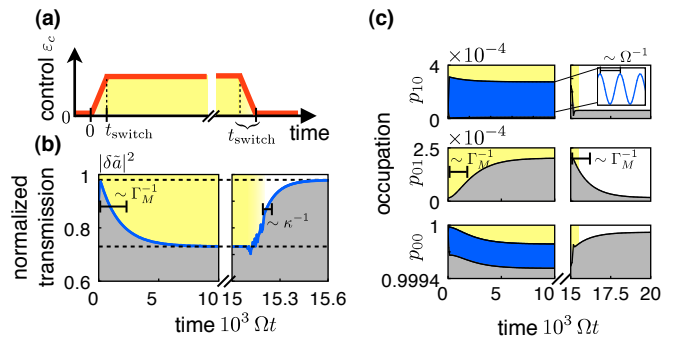

Figure 3: Optomechanical transistor for large g_0/κ. (a) The probe drives the cavity continuously. At time $t = 0$, the control laser power is ramped-up linearly until $\Omega t_{\text{switch}} \gg 1$. This decreases the normalized probe beam transmission on a scale $\sim \Gamma_M^{-1}$, cf. (b). When switching off the control linearly, $|\delta\tilde{a}|^2$ increases on a scale $\sim \kappa^{-1} \ll \Gamma_M^{-1}$. (c) Occupation transfer between individual quantum states induced by the control. Oscillations at Ω are clearly visible in p_{10} (i.e. for the state with 1 photon, 0 phonons). [Parameters: same as in Fig. 2, $\Delta_p = 0$, $\Omega t_{\text{switch}} = 100$].

nominator of (6) is changed in this regime [19]. When taking these modifications into account in (6) we obtain quantitative agreement, cf. Fig. 2(b).

Thus, the standard OMIT dip in the nonlinear quantum regime is still controlled by the photon number $\langle \hat{a}^\dagger \hat{a}\rangle$ only, allowing the operation of an optomechanical transistor in a pulsed scheme.

Optomechanical transistor – Let us consider a resonant probe beam. At $t = 0$, we ramp-up the control power linearly (to avoid spurious transients). At $\Omega t_{\text{switch}} \gg 1$, the red detuned control $(\Delta_c = -\Omega)$ reaches its maximum power, cf. Fig. 3(a). This decreases the probe beam transmission $|\delta\tilde{a}|^2$ on a timescale set by the OMIT dip's width $\sim \Gamma_M^{-1}$. When reaching the steady state, the control beam is linearly switched off. Then, $|\delta\tilde{a}|^2$ increases rapidly on a scale $\sim \kappa^{-1}$, cf. Fig. 3(b), because control photons decay out of the cavity on this timescale. The influence of the control can also be seen in the population p_{n_a,n_b} of the states $|n_a, n_b\rangle$, cf. Fig. 3(c). Control and probe together first increase the population of the one-photon state $|1,0\rangle$. Then, on a scale $\sim \Gamma_M^{-1}$, the one-phonon state's population $p_{0,1}$ increases, thus $|\delta\tilde{a}|^2$ decreases. Furthermore, population between the zero and one photon ladder is exchanged coherently, leading to oscillations at $\omega_p - \omega_c = \Omega$.

Quantum to classical crossover – We now discuss how signatures of the quantum nonlinearity could be observed using OMIT even if the coupling strength $g_0 < \kappa$, which is relevant for present experiments. As discussed above, to distinguish nonlinear quantum effects from classical effects, we study the OMIT signal as a function of the
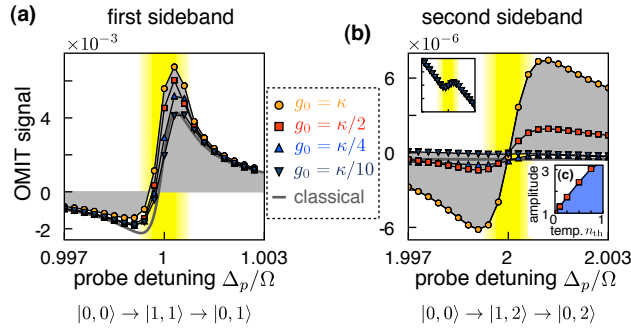
Figure 4: Quantum to classical crossover. The OMIT signal at the second sideband (b) vanishes in the classical limit $g_0/\kappa \to 0$, hence being a clear signature of the quantum nonlinearity. It is visible even for moderate coupling strengths $g_0 < \kappa$. The yellow regions indicate the OMIT features's width $\sim \Gamma_M$. (a) Since $\Delta_p = \Omega$ and $\Delta_c = 0$, probe and control couple the levels $|0,0\rangle \leftrightarrow |1,1\rangle$ and $|0,1\rangle \leftrightarrow |1,1\rangle$ respectively. (b) Since $\Delta_p = 2\Omega$ and $\Delta_c = 0$, $|0,0\rangle \leftrightarrow |1,2\rangle$ and $|0,2\rangle \leftrightarrow |1,2\rangle$ are coupled, respectively. Symbols: OMIT signal for different g_0/κ where $g_0|\alpha|$ and κ are kept fixed. Grey line: classical expectation, cf. (6). Inset of (b): OMIT signal for $g_0/\kappa = 1/10$. The axis are the same as in (b). The OMIT signal varies in a range $\sim 10^{-7}$. Note that the signal strength can be increased by increasing $g_0|\alpha|$. (c) Amplitude of the Fano resonance at the second sideband (i.e. the difference between the maximum and minimum) versus the thermal phonon number n_{th} (normalized to the amplitude at $n_{th} = 0$). [Parameters: $\kappa = \Omega/8$, $\Gamma_M = 10^{-3}\Omega$, $\Delta_c = 0$, $n_{th} = 0$, $g_0\varepsilon_c = 1.25 \cdot 10^{-3}\Omega^2 = $ const. (This value has been chosen to keep the Hilbert space manageable as $g_0/\kappa \to 0$). (c): Same as in (b), $g_0/\kappa = 1/2$]

quantum parameter g_0/κ while keeping the classical prediction (6) unchanged.

The most significant signature of the quantum nonlinearity can be obtained for a resonant control beam, i.e. $\Delta_c = 0$ and observing the OMIT signal close to the mechanical sidebands, i.e. $\Delta_p \approx n\Omega$, where $n = 1, 2, \ldots$.

At the first mechanical sideband ($n = 1$), the classical theory (6) predicts a Fano-resonance, cf. Fig. 4(a). Fano resonances in general have recently been discussed in the context of optomechanics [35–39]. The Fano resonance emerges because the probe beam probes both the first order, off-resonant $|1,0\rangle \leftrightarrow |0,0\rangle$ transition plus the second-order, resonant transition $|0,1\rangle \leftrightarrow |0,0\rangle$, the latter being a joint effect of the probe and control. For small quantum parameters $g_0 \ll \kappa$, the OMIT signal converges to the classical expectation. Upon increasing g_0/κ, the Fano resonance becomes slightly more pronounced as the relevant $|0,0\rangle \leftrightarrow |1,1\rangle$ transition becomes more likely due to the Franck Condon factor $\sim (g_0/\Omega)$ (in leading order). Note that the strength of the OMIT signal can be increased by increasing $g_0|\alpha|$.

Second sideband OMIT as a sensitive probe – Let us consider the second mechanical sideband, $\Delta_p \approx 2\Omega$,

while, again, $\Delta_c = 0$, cf. Fig. 4(b). The classical analysis (whether linearized or fully nonlinear [31]) fails to show an OMIT signature here, because it does not capture transitions to sidebands $n > 1$. However, when including the quantum nonlinearity, OMIT signatures do exist. These vanish in the classical limit $g_0/\kappa \to 0$ and are thus solely due to the quantum nonlinearity.

This feature emerges due to the two-photon transition $|0,0\rangle \mapsto |1,2\rangle \mapsto |0,2\rangle$, with additional interference of off-resonant transitions probed by the probe beam. The two-photon transition is enabled due to shifted phonon states. Importantly, we observe this significant feature even for moderate coupling $g_0 = \kappa/10$ (in contrast to other quantum signatures which require $g_0 > \kappa$ [19, 25]). The OMIT signal increases with increasing g_0/κ. This is because the relevant higher order sideband transition rates increase due to an increase of the Franck-Condon factors with g_0. Thus, we predict that a two-tone driving experiment should be able to identify quantum signatures of the optomechanical interaction even for moderate single-photon coupling strengths $g_0 < \kappa \ll \Omega$.

We now discuss the influence of temperature on the OMIT signal at the second sideband, cf. Fig. 4(c). As we increase temperature, we find that the Fano resonance amplitude even increases, while the dependence on g_0/κ indicates that the effect is still a signature of quantum nonlinearities, vanishing in the classical limit. A possible explanation is that higher phonon states are now thermally occupied. Thus, the transitions $|0, n_b\rangle \leftrightarrow |1, n_b + 2\rangle$ with $n_b > 0$ are additionally probed. The corresponding Franck-Condon factors increase with n_b (if $g_0 \ll \Omega$), leading to the observed enhancement.

We now discuss what happens as we increase the probe driving strength ε_p. We find that even for $\varepsilon_p \sim \varepsilon_c$ the OMIT signal does not change. The probe beam drives the cavity on the second sideband and thus the number of probe photons inside the cavity is still much lower than the number of control photons (as long as $\varepsilon_p/\varepsilon_c \ll \Omega/\kappa$) - the probe is still a small perturbation. This is experimentally relevant, since one can therefore increase the absolute probe transmission by increasing the probe intensity. This also holds for the first mechanical sideband (but not for the main OMIT dip, where the OMIT signal begins to be suppressed even for $\varepsilon_p/\varepsilon_c \sim \kappa/\Omega$).

We conclude that the challenge to bring out nonlinear quantum signatures in optomechanical systems will be greatly aided by two-tone driving.

Note added: While preparing this manuscript for upload, two related works appeared on the arXiv [40, 41].

* Electronic address: andreas.kronwald@physik.uni-erlangen.de

[1] P. Meystre, Annalen der Physik **525**, 215 (2013).

[2] M. Aspelmeyer, T. J. Kippenberg, and F. Marquardt, arXiv:1303.0733 .

[3] G. S. Agarwal and S. Huang, Phys. Rev. A **81**, 041803 (2010).

[4] S. Weis, R. Rivière, S. Deléglise, E. Gavartin, O. Arcizet, A. Schliesser, and T. J. Kippenberg, Science **330**, 1520 (2010).

[5] J. D. Teufel, D. Li, M. S. Allman, K. Cicak, A. J. Sirois, J. D. Whittaker, and R. W. Simmonds, Nature **471**, 204 (2011).

[6] A. H. Safavi-Naeini, T. P. M. Alegre, J. Chan, M. Eichenfield, M. Winger, Q. Lin, J. T. Hill, D. E. Chang, and O. Painter, Nature **472**, 69 (2011).

[7] F. Massel, T. T. Heikkila, J.-M. Pirkkalainen, S. U. Cho, H. Saloniemi, P. J. Hakonen, and M. A. Sillanpaa, Nature **480**, 351 (2011).

[8] M. Fleischhauer, A. Imamoglu, and J. P. Marangos, Rev. Mod. Phys. **77**, 633 (2005).

[9] K. W. Murch, K. L. Moore, S. Gupta, and D. M. Stamper-Kurn, Nat Phys **4**, 561 (2008).

[10] F. Brennecke, S. Ritter, T. Donner, and T. Esslinger, Science **322**, 235 (2008).

[11] D. W. C. Brooks, T. Botter, S. Schreppler, T. P. Purdy, N. Brahms, and D. M. Stamper-Kurn, Nature **488**, 476 (2012).

[12] J. D. Teufel, T. Donner, D. Li, J. W. Harlow, M. S. Allman, K. Cicak, A. J. Sirois, J. D. Whittaker, K. W. Lehnert, and R. W. Simmonds, Nature **475**, 359 (2011).

[13] J. Chan, T. P. M. Alegre, A. H. Safavi-Naeini, J. T. Hill, A. Krause, S. Groblacher, M. Aspelmeyer, and O. Painter, Nature **478**, 89 (2011).

[14] E. Verhagen, S. Deleglise, S. Weis, A. Schliesser, and T. J. Kippenberg, Nature **482**, 63 (2012).

[15] J. Chan, A. H. Safavi-Naeini, J. T. Hill, S. Meenehan, and O. Painter, Applied Physics Letters **101**, 081115 (2012).

[16] S. Mancini, V. I. Man'ko, and P. Tombesi, Phys. Rev. A **55**, 3042 (1997).

[17] S. Bose, K. Jacobs, and P. L. Knight, Phys. Rev. A **56**, 4175 (1997).

[18] M. Ludwig, B. Kubala, and F. Marquardt, New Journal of Physics **10**, 095013 (2008).

[19] A. Nunnenkamp, K. Børkje, and S. M. Girvin, Phys. Rev. Lett. **107**, 063602 (2011).

[20] J. Qian, A. A. Clerk, K. Hammerer, and F. Marquardt, Phys. Rev. Lett. **109**, 253601 (2012).

[21] X.-W. Xu, H. Wang, J. Zhang, and Y. xi Liu, arXiv:1210.0070 .

[22] J. Li, S. Gröblacher, and M. Paternostro, New Journal of Physics **15**, 033023 (2013).

[23] A. Nunnenkamp, K. Børkje, and S. M. Girvin, Phys. Rev. A **85**, 051803 (2012).

[24] G.-F. Xu and C. K. Law, Phys. Rev. A **87**, 053849 (2013).

[25] P. Rabl, Phys. Rev. Lett. **107**, 063601 (2011).

[26] A. Kronwald, M. Ludwig, and F. Marquardt, Phys. Rev. A **87**, 013847 (2013).

[27] K. Stannigel, P. Komar, S. J. M. Habraken, S. D. Bennett, M. D. Lukin, P. Zoller, and P. Rabl, Phys. Rev. Lett. **109**, 013603 (2012).

[28] M. Ludwig, A. H. Safavi-Naeini, O. Painter, and F. Marquardt, Phys. Rev. Lett. **109**, 063601 (2012).

[29] A. Xuereb, C. Genes, and A. Dantan, Phys. Rev. Lett. **109**, 223601 (2012).

[30] A. Schließer, *Cavity Optomechanics and Optical Frequency Comb Generation with Silica Whispering-Gallery-Mode Microresonators*, Ph.D. thesis (2009).

[31] H. Xiong, L.-G. Si, A.-S. Zheng, X. Yang, and Y. Wu, Phys. Rev. A **86**, 013815 (2012).

[32] C. K. Law, Phys. Rev. A **51**, 2537 (1995).

[33] A. A. Clerk, M. H. Devoret, S. M. Girvin, F. Marquardt, and R. J. Schoelkopf, Rev. Mod. Phys. **82**, 1155 (2010).

[34] C. Gardiner and P. Zoller, *Quantum Noise* (Springer, 2004).

[35] D. A. Rodrigues, Phys. Rev. Lett. **102**, 067202 (2009).

[36] F. Elste, S. M. Girvin, and A. A. Clerk, Phys. Rev. Lett. **102**, 207209 (2009).

[37] A. Xuereb, R. Schnabel, and K. Hammerer, Phys. Rev. Lett. **107**, 213604 (2011).

[38] T. Weiss, C. Bruder, and A. Nunnenkamp, New Journal of Physics **15**, 045017 (2013).

[39] K. Qu and G. S. Agarwal, Phys. Rev. A **87**, 063813 (2013).

[40] M.-A. Lemonde, N. Didier, and A. A. Clerk, Phys. Rev. Lett. **111**, 053602 (2013).

[41] K. Børkje, A. Nunnenkamp, J. D. Teufel, and S. M. Girvin, Phys. Rev. Lett. **111**, 053603 (2013).